Article:
Parks, C.M., Meijer, A.J.H.M., Blakey, S.G. et al. (2022) Computational studies on the reactions of thiols, sulfides and disulfides with hydroperoxides. Relevance for jet fuel autoxidation. Fuel, 316. 123326. ISSN: 0016-2361

https://doi.org/10.1016/j.fuel.2022.123326

Computational studies on the Reactions of Thiols, Sulfides and Disulfides with Hydroperoxides. Relevance for Jet Fuel Autoxidation.

*Christopher M. Parks** [a], *Anthony J.H.M. Meijer*[b], *Simon G. Blakey,* [c] *Ehsan Alborzi* [a] *Mohamed Pourkashanian*[a]

[a] *Department of Mechanical Engineering, The University of Sheffield, Sheffield S3 7RD,UK*

[b] *Department of Chemistry, The University of Sheffield, Sheffield, S3 7HF*

[c] *Department of Mechanical Engineering, The University of Birmingham, Birmingham B15 2TT, U.K.*

Email: c.m.parks@sheffield.ac.uk, e.alborzi@sheffield.ac.uk, S.G.Blakey@bham.ac.uk, a.meijer@sheffield.ac.uk

Abstract

Density Functional Theory calculations (DFT) are reported on the reactions of hydroperoxides with different classes of sulfur: thiols (RSH), sulfides (RSR) and disulfides (RSSR), all of which are important trace species in the auto-oxidation of jet fuel. It is shown that thiols can react under auto-oxidation conditions with hydroperoxides to form sulfonic acids and alcohols. In contrast, it is shown that disulfide species are more likely to form thiyl radicals, which are

less likely to be important for the direct autoxidation of fuels due to prohibitive reaction barriers. The reaction mechanisms reported here for sulfur oxidation and the associated calculated thermodynamic data can be used to extend the applicability of current chemical kinetic models for fuel autoxidation, which are currently treated as a single elementary reaction despite the range of sulfur species found in fuels.

Keywords: DFT, Fuel autoxidation, Sulfur oxidation, Reaction Mechanisms.

Introduction

Jet fuel is primarily comprised of a blend of aliphatic and aromatic hydrocarbons as well as low levels of hydroperoxides and trace heteroatomic species (the latter generally in ppm quantities). The hydrocarbons afford the fuel its bulk properties such as viscosity, density and volatility which are not only important when it is used as a propellant, but also when exploited as a coolant as happens in modern aircraft. In the latter use, at temperatures of approximately 140 $^{\circ}$C a process called autoxidation is initiated. Here a series of chemical reactions can occur that can lead to both bulk and surface deposits. Experimentally, it has been shown that many species can have an effect on this process including sulfur compounds[1-3], polar species[4-9], dissolved metals[10, 11] and hydroperoxides.[12, 13] A number of studies have reported on the thermal stability of jet fuel, with a focus on the oxidative mechanisms involved therein.[14-21]

In the current paper, we focus on the reactions between sulfur species and hydroperoxides. A number of different classes of sulfur compounds can be present in jet fuels as shown in **Figure**

1. They include thiols (RSH), sulfides (RSR), disulfides (RSSR), thiophenes, benzothiophenes, dibenzothiophenes and substituted variants thereof. Oxidized variants of these such as sulfoxides and sulfonic acids can either be present initially or formed through reactions with oxygen and hydroperoxides. Multiple studies have focused on classifying the types of sulfur species present in aviation fuel. In these studies, several analytical techniques were employed to separate sulfur species from aviation fuels and gasolines. They were subsequently classified as reactive and non-reactive sulfurs and further subcategorized as thiols, sulfides, disulfides, thiophenes, benzothiophenes and substituted benzothiophenes.[22-24] .

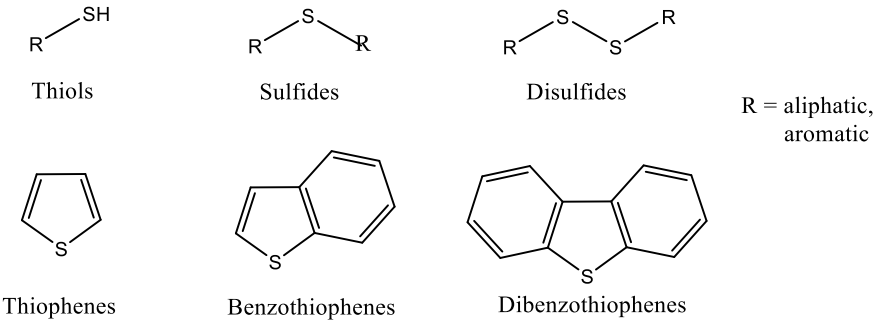

Figure 1: General structures of common sulfur species found in jet fuel.

The exact nature of the role of sulfur in jet fuel is still being debated in the literature. Indeed, there are a number of reviews on the subject with contrasting views.[8, 25-29] Irrespective of this debate, it has been accepted that sulfur species react with hydroperoxides in the fuel as in **Figure 2**. This sulfur-hydroperoxide reaction proceeds *via* a non-radical mechanism to form oxidized sulfur compounds and alcohols.[30] This process results in a reduction in the hydroperoxide concentration, which could in turn retard the rate of autoxidation of the fuel.

Figure 2: Reaction of hydroperoxides and sulfides to form alcohols and sulfones. (R = aliphatic, aromatic)

A number of literature studies have reported on the effects of sulfur species on jet fuel autoxidation. In 1976, Taylor showed that thiophenes and disulfide species contribute significantly to deposition.[8] Moreover, dibenzothiophenes were found to have little effect on deposition. These observations were further corroborated by Mushrush et al. who showed that thiophenes and thiophenols have a destabilizing effect on jet fuel.[29] Further work by Offenhauer and Hiley showed that both sulfonic acids and thiophenols increased both deposition and gum formation whereas diaryl sulfides have little effect.[31, 32] The proposed dual roles that sulfur compounds can play was reported by both Denison et al. and Thompson et al..[33, 34] They observed that disulfides decreased the thermal stability of the fuel. In contrast, aliphatic sulfides had a small stabilizing effect. In a series of experimental studies, Daniel and Henemen doped jet fuel with different sulfur species at a range of concentrations.[35] Thiols and thiophenes decreased the thermal stability whilst disulfides and sulfides increased the thermal stability. The largest amount of deposits were observed by Rawson et al. for model fuels doped with benzylsulfonic acid, diphenyl disulfide and elemental sulfur.[36] The contrasting results in many of these studies highlight the complex nature of the underlying mechanisms.

Despite the importance of these trace sulfur species in jet fuel, there has only been a limited number of computational studies into the energetics of the reactions involving these species. Bach and co-workers investigated the activation energy for the reaction of Me_2S with

methylperoxide (MeOOH) and tert-butyl peroxide (^{t}BuOOH), which were calculated to be 32.4 and 32.2 kcal mol^{-1} respectively.[37] In these calculations it was shown for the first time that the transition state is concerted. In particular, the hydroxyl oxygen atom in the hydroperoxide is transferred to the sulfur as the hydrogen moves to form the alcohol. More recently, Zabarnick et al. modelled the reactions of Et_2S and EtSSEt with ^{n}BuOOH.[30] The activation energies for these reactions were 26.1 and 28.7 kcal mol^{-1}.

The lack of detailed investigations into the reactions of sulfur compounds and hydroperoxides prompted our investigation. Current chemical kinetic models, which aim to predict the rate of fuel autoxidation describe sulfur chemistry using one elementary reaction (**equation 1**).[10] Given the wide range of sulfur species that could be present in jet fuels, it is likely that the applicability of such kinetic models could be improved by a more through understanding of the individual reactions each sulfur species could undergo.

$$SH + ROOH \longrightarrow Products_{SH}{}^{10} \quad (1)$$

In this paper, we report on a series of DFT calculations on a large range of sulfur compounds, which are each in turn reacting with multiple hydroperoxides. Further reactions beyond the initial oxidation are considered. The different routes to the formation of sulfones and sulfonic acids are also probed. The propensity of disulfide species to undergo fission reactions and form thiyl radicals are also investigated as are the potential implications of the formation of such species. In its entirety, our work provides an extensive thermochemical library for sulfur–peroxide reactions to further improve current kinetic models for aviation fuel degradation.

2 Experimental and computational Details

An analysis of a sample of Jet A-1 fuel was conducted in order to determine which sulfur species were the most appropriate to model. Jet A-1 fuel samples were analysed for sulfur content using an in-house method. This method identifies the sulfur species in middle distillates using an Agilent 7890N Gas chromatogram combined with a Zoex thermal modulation and chemiluminescence detector. Quantification of the types of sulfur species present was achieved through normalization against the total sulfur content of the fuel sample as determined by combustion followed by UV fluorescence analysis. This analytical method separates all the sulfur-containing compounds according to their boiling point and polarity. This afforded the ability to differentiate between benzothiophenes and dibenzothiophenes observed as two well-defined bands, which were well separated from the lower polarity thiophenes, mercaptans and sulfides.[38-40]

DFT calculations were performed using Gaussian 09 software[41], version D.01, using Gaussian-supplied versions of BLAS and ATLAS.[42, 43] All calculations used the B3LYP functional.[44-46] The cc-pVTZ basis set was used for all elements.[47] Benchmarking studies show this setup to be acceptable.[16, 19] In all calculations solvent was accounted for by the polarizable continuum model (PCM) method using solvent parameters for dodecane as implemented in Gaussian.[48, 49] Calculations were carried out at 298.15 K. Geometry optimizations were confirmed to be local minima by the absence of imaginary frequencies in the vibrational spectra. Transition states were optimized using the QST3 method as implemented in Gaussian.[50] All transition states were confirmed both visually *via* the presence of one large imaginary frequency corresponding to the saddle point and *via* intrinsic reaction coordinate (IRC) scans. An ultrafine grid was employed for all calculations with no symmetry constraints. Radical species were calculated

as singlets with the HOMO and LUMO orbitals mixed (guess=mix option) in order to break the symmetry of the system. Free energies were calculated using the Grimme quasiharmonic entropy correction using the GoodVibes script.[51] Selected stationary points were improved with coupled cluster calculations (CCSD(T)) using MolPro.[52] Quoted values in the manuscript are subject to an error of ± 2.5 kcalmol^{-1} based upon benchmarking studies. [16, 19]

Activation energies are calculated as the energy difference between the transition state and both reactants at infinite separation. Arrhenius pre-exponential factors were calculated according to **equation 2**.

$$A = \frac{k_b T}{h} exp\left(\frac{\Delta S}{R}\right) \quad (2)$$

3 Results and Discussion

3.1 Sulfur selection

Table 1: Results from the analysis of sulfur content in a Jet A-1 fuel sample

Sulfur species	Amount detected / %
Thiols, sulfides and disulfides	57
Dibenzothiophenes	26
Unknown	12
Dibenzothiophenes	2
Benzothiophenes	2
Substituted dibenzothiophenes	1

In order to guide our computational investigations, we initially conducted a speciation analysis of a JetA-1 fuel using GC x GC as described in the experimental section. The results of this analysis are shown in **Table 1.** By far, the most abundant sulfur species detected were thiols, disulfides and sulfides (57 %). These were followed by substituted benzothiophenes (26.0 %)

and dibenzothiophenes (12.0 %). A small quantity of non-substituted benzothiophenes were also detected. Based upon these observations, the species shown in **Figure 3** were selected for computational analysis. For thiols, sulfides and disulfides a mixture of aromatic and aliphatic R groups were selected. These were chosen to provide as wide a selection of structures as possible within the range of compounds detected in the jet fuel sample.

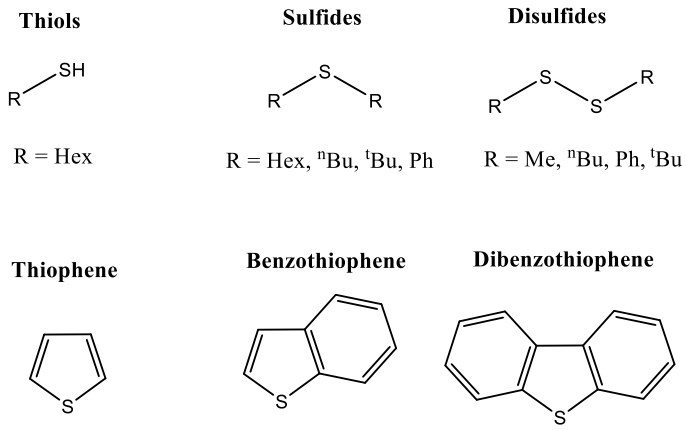

Figure 3: Structures of sulfur species selected for computational analysis

3.2 Reactions of thiols and sulfides with hydroperoxides

Our computational studies were initially focused on how the aforementioned sulfur species might affect autoxidation by investigating how they react with hydroperoxides. It has previously been reported that sulfur species react with hydroperoxides to form alcohols and oxidized sulfur species through a non-radical pathway.[29] Our initial studies focused on the reactions of thiols (general formula RSH). The energy profile for the reaction of hexane thiol and methyl hydroperoxide is shown in **Figure 4**.

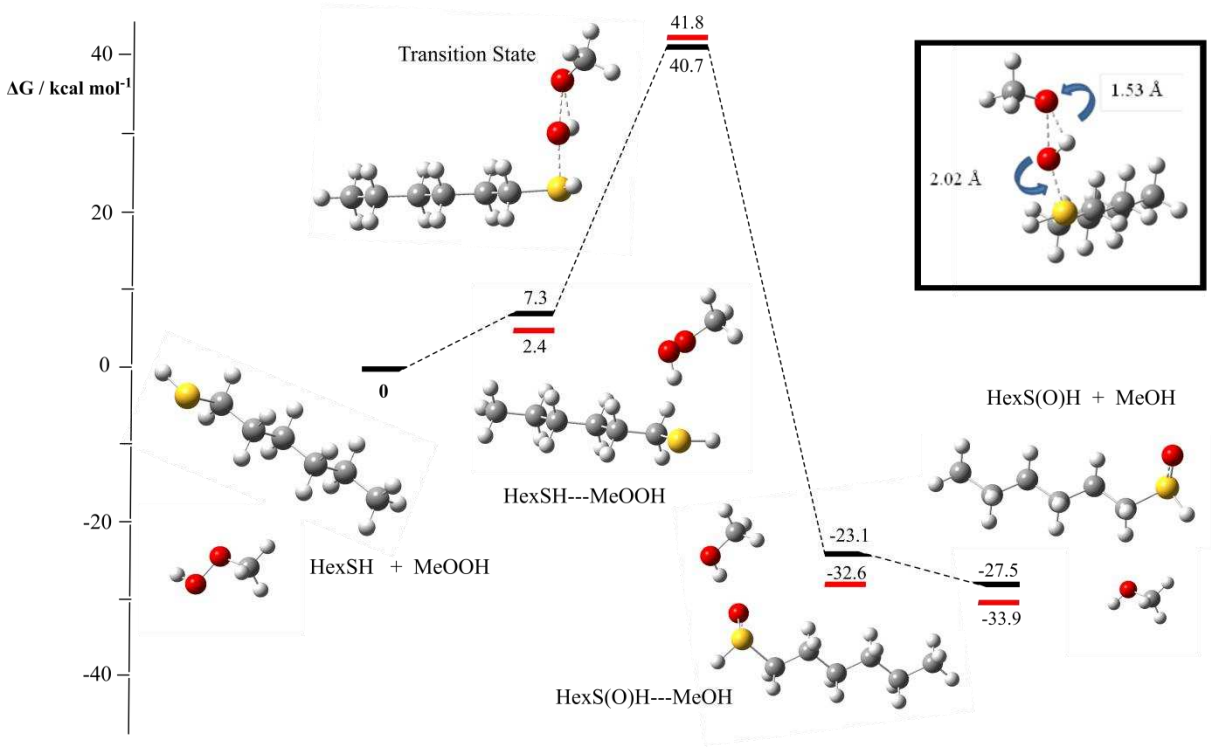

Figure 4: Gibbs free energy profile for the reaction of hexane thiol and MeOOH. Inset: Transition state structure. Results from CCSD(T) calculations shown in red.

The pre-reaction complex, (HexSH---MeOOH in **Figure 4**) is defined as the structure where the two reactants are in close proximity immediately prior to the reaction taking place. Here, the pre-reaction complex is 7.3 kcal mol^{-1} less stable than the separated reactants. The transition state geometry is shown inset in **Figure 4.** The hydroxyl oxygen of the incoming hydroperoxide is transferred to the sulfur atom of the thiol. Concurrently, the hydroxyl hydrogen is transferred back to form an alcohol. The activation free energy for this reaction is 40.7 kcal mol^{-1} and the reaction free energy is -27.5 kcal mol^{-1}.

Next, we considered the effect of the chosen hydroperoxide on the activation energy. It is computationally efficient to conduct these calculations using MeOOH as a model for the hydroperoxides found in jet fuel. However, it is not a representative structure. Fuel hydroperoxides will contain a much longer carbon chain or could be derived from branched

paraffinic species. Therefore, we investigated the reactions with different hydroperoxides to ascertain whether MeOOH was an appropriate model. To address this, we calculated the same energy profile as shown in **Figure 4**, replacing MeOOH with a range of linear alkyl peroxides (Carbon numbers 1 to 12) and two branched hydroperoxides – cumene hydroperoxide (CHP) and ^{t}BuOOH. The effect on the activation energy and reaction energy of increasing chain length is presented in **Figure S3** in the supporting information.

As can be seen from **Figure S3**, the effect of increasing the hydroperoxide chain length on both the activation free energy and reaction free energy is small. In particular, activation free energies range from 40.7 - 42.4 kcal mol^{-1}. Reaction free energies range from -33.6 to -34.3 kcal mol^{-1}). A reduction in the activation free energy to 39.95 kcal mol^{-1} is noted when CHP is used as the model hydroperoxide. The corresponding value for ^{t}BuOOH is 41.5 kcal mol^{-1}. In light of these results, further studies hereafter are carried out using both MeOOH, ^{t}BuOOH and CHP. MeOOH was chosen as it clearly is an acceptable model for the larger linear-chained hydroperoxides. Moreover, it can be modelled in a timely manner. CHP and ^{t}BuOOH were chosen as more realistic fuel peroxides for aromatic and branched hydroperoxides respectively. Data for the reactions of sulfur species and both ^{t}BuOOH and CHP can be found in the supporting information and is collated in **Table 3**.

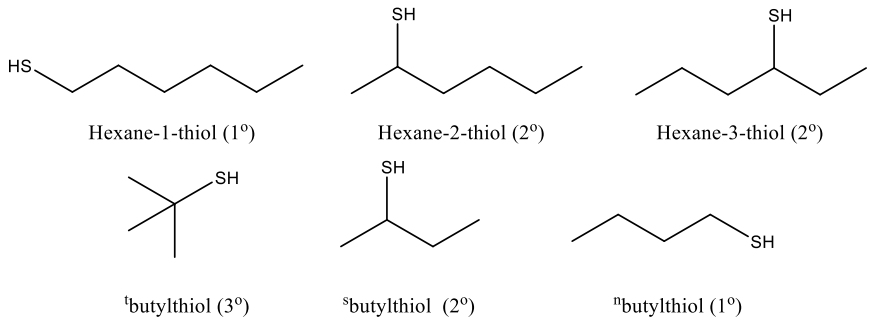

Figure 5: Primary (1°), secondary (2°) and tertiary (3°) thiol species selected for investigation

Consideration was also given as to how branching in the sulfur species affects the reactivity with hydroperoxides. Several sulfur species were selected for investigation as shown in **Figure 5**, containing primary, secondary and tertiary thiols. In each case, the reaction with MeOOH was modelled. The Gibbs free activation and reaction energies are collated in **Table 2**. As can be seen, branching of the carbon chain has a minimal effect on both the Gibbs free activation and reaction energies for the first oxidation reaction. This suggests that, at least for thiols containing only carbon chains and no further functional groups, linear thiols can be investigated as model complexes.

Table 2: Collated Gibbs free activation and reaction energies for the reaction of primary (1^o), secondary(2^o) and tertiary thiols (3^o) and MeOOH.

Sulfur species (type)	**Gibbs free activation energy / kcal mol^{-1}**	**Gibbs reaction energy / kcal mol^{-1}**
Hexane-1 thiol (1^o)	41.8	-27.5
Hexane-2 thiol (2^o)	40.9	-27.0
Hexane-3 thiol (2^o)	42.6	-25.7
^{n}butylthiol (1^o)	41.8	-25.7
^{s}butylthiol (2^o)	40.8	-28.0
^{t}butylthiol (3^o)	40.4	-29.1

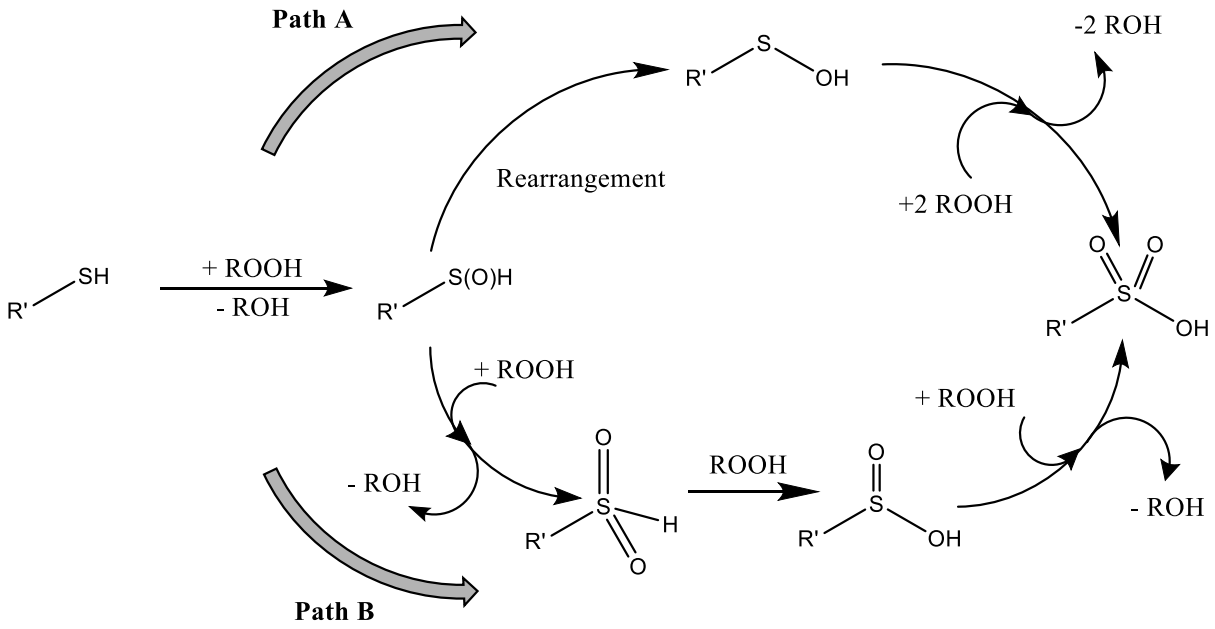

Scheme 1: Two potential mechanistic pathways leading to formation of RS(O)(O)OH.

Having considered the effect of both branching in the sulfur species and how the hydroperoxide chain length affects the reactivity, we turned our attention to the subsequent reactions that the oxidized thiol can undergo. The reaction of hexanethiol and MeOOH from **Figure 4** initially forms an oxidized sulfur species (RS(O)H) and an alcohol. Through successive further oxidations it can form a sulfonic acid (RS(O)(O)OH). This can occur through two distinct routes as illustrated in **Scheme 1**. The oxidized sulfur species can first rearrange to form a sulfenic acid (RSOH) which can subsequently undergo two further oxidation reactions with hydroperoxides to form the sulfonic acid (**path A** in **Scheme 1**). Alternatively, two further oxidation reactions can occur either side of a rearrangement to form RS(O)(O)OH (**path B** in **Scheme 1**). The energy profile illustrating the two divergent pathways starting from RS(O)H-- --ROOH is presented in **Figure 6.**

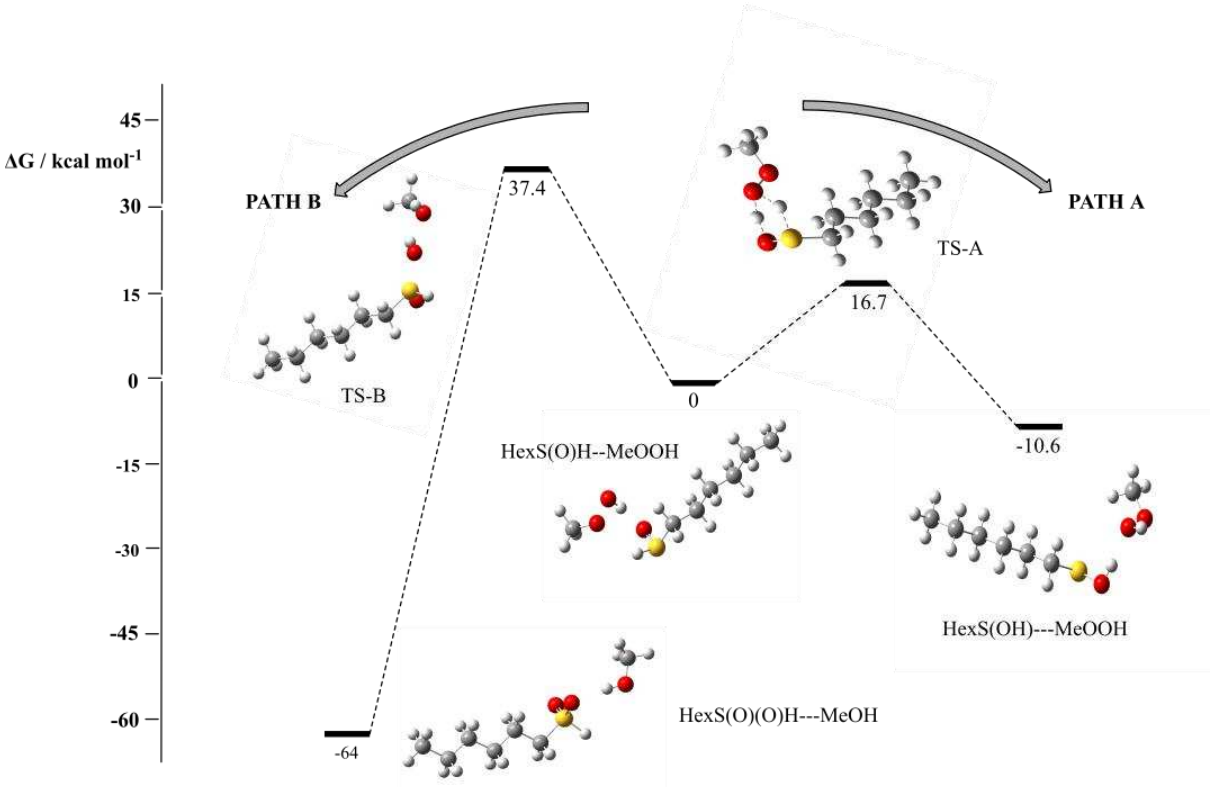

Figure 6: Gibbs free energy profile illustrating the two reactions that oxidized hexanethiol can undergo with MeOOH.

The activation free energy for the oxidation of HexS(O)H to HexS(O)(O)H is 37.4 kcal mol^{-1}. (**path B** in **Figure 6**) This is significantly larger than the activation free energy for re-arrangement to form a sulfenic acid, HexS(OH) (16.7 kcal mol^{-1}). Thus, the calculation suggests that re-arrangement occurs prior to further oxidation. Activation free energies for subsequent oxidations starting from a sulfenic acid are 23.1 kcal mol^{-1} and 33.1 kcal mol^{-1} for the transformation of HexSOH to HexS(O)(O)H and HexS(O)(O)H to HexS(O)(O)OH respectively. This data is provided in the supporting information.

We note that in a recent publication, we showed that the concentration of hydroperoxides decreases significantly with each successive oxidation.[53, 54] As a consequence, each successive oxidized sulfur species will be present in a much lower concentration than the initial non-

oxidized sulfur compound. Thus, it is likely that only the initial oxidation reaction will be important in jet fuel given that further oxidation reactions will occur with a low frequency. Of course, the significance of each successive reaction may increase for fuels containing a higher concentration of hydroperoxides.

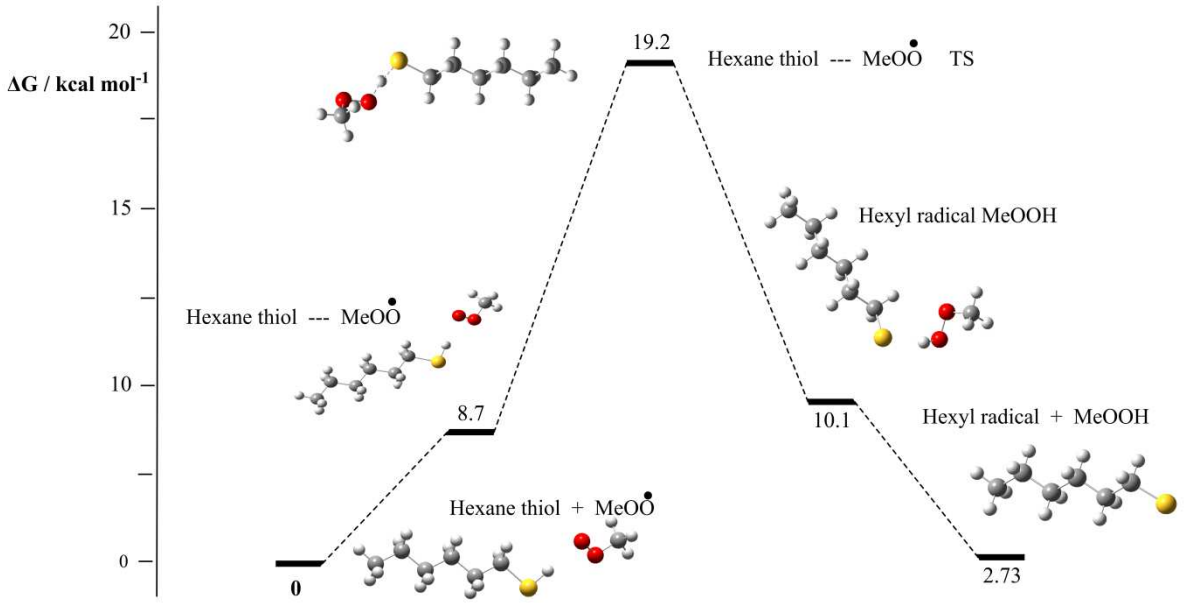

Figure 7: Gibbs free energy profile for the reaction of hexanethiol and MeOO●.

Our final consideration regarding thiol reactivity concerned the possibility of thiols reacting with peroxy radicals. Given that sulfur species have been shown to produce widely varying effects on jet fuel autoxidation and deposition, it is likely that they react with more than just hydroperoxides. Consequently, we investigated the reaction of hexane thiol and MeOO●. The Gibbs free energy profile is shown in **Figure 7**. This reaction has a free activation energy of 19.2 kcal mol^{-1} and the overall reaction is only marginally uphill. This data suggests that thiols can react with peroxy radicals and generate hydroperoxides and thiyl radicals. Further investigations of the reactions that thiyl radicals can undergo will be detailed in **section 3.4**.

Sulfides were the next class of compounds to be investigated. Sulfides have the general formula RSR. They can undergo similar reactions with hydroperoxides as observed for thiols. However, in this case, there is a maximum of two oxidation steps. Moreover, sulfenic acid cannot be formed because there is no terminal –SH bond. The free energy profile for the reaction of hexyl sulfide and MeOOH is shown in **Figure 8.**

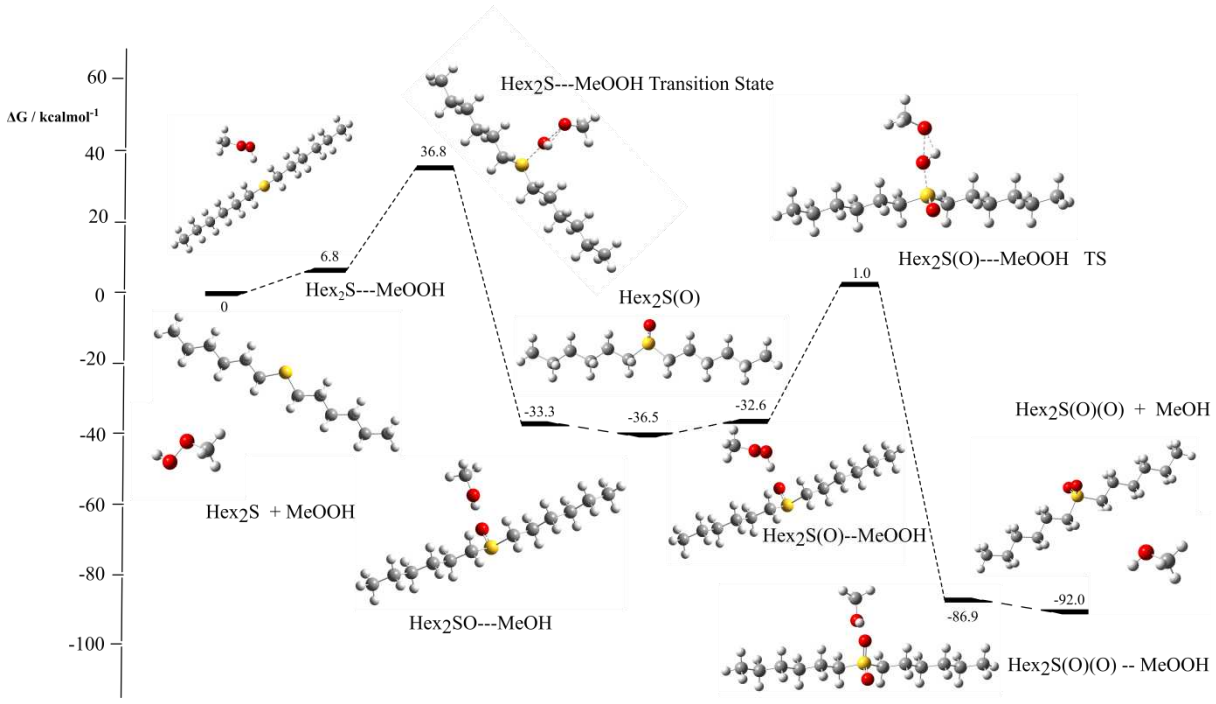

Figure 8: Gibbs free energy profile for the reaction of hexylsulfide and MeOOH.

The activation free energy for the oxidation of Hex_2S to $Hex_2S(O)$ is 36.8 kcal mol^{-1}, which is similar to the activation free energy for the oxidation of hexane thiol. The second oxidation reaction has an activation free energy of 37.5 kcal mol^{-1}. Both of these reactions are permissible given the standard conditions experienced during autoxidation (temperatures of between 140 and 300 °C). Corresponding activation energies for the reaction of CHP and Hex-S-Hex are 36.7 kcal mol^{-1} and 37.4 kcal mol^{-1} for the conversion of Hex_2S to $Hex_2S(O)$ and $Hex_2S(O)$ to $Hex_2S(O)(O)$ respectively.

Table 3: Collated Gibbs free activation energies for the first and second oxidation reactions between three sulfides and MeOOH.

Sulfur species	Gibbs free activation energy / kcal mol^{-1}	
	First oxidation	Second oxidation
phenylsulfide	39.3	39.3
^{n}butylsulfide	36.6	37.4
^{t}butylsulfide	35.3	35.0

Table 3 contains calculated Gibbs free activation energies for the reaction of three further sulfides with MeOOH. The chosen sulfides contained phenyl, ^{n}butyl and ^{t}butyl substituents. As can be seen in **Table 3**, the first and second oxidation reactions of ^{n}butylsulfide and MeOOH are very similar to those calculated in **Figure 8**. As the only change between ^{n}butylsulfide and hexylsulfide is a reduction in the carbon chain length, this result is to be expected. The first and second oxidation reactions of phenylsulfide and MeOOH are higher than those reported for hexylsulfide

3.3 Reactions of thiophenes, benzothiophenes and dibenzothiophenes

The speciation analysis that we carried out on jet fuel indicated that substituted benzo- and dibenzothiophenes were the most observed species after thiols, sulfides and disulphides. However, the analysis did not provide information as to the exact nature and location of the substitutions. Due to this, we next investigated non-substituted analogues (ie, thiophene, benzothiophene and dibenzothiophenes) as models for these species.

Figure 9 shows the calculated energy profile for the reaction of thiophene and MeOOH. Thiophene can undergo two successive oxidations with hydroperoxides as was the case for

sulfides (RSR). The activation free energy for the oxidation of thiophene to thiophene(O) is 48.3 kcal mol^{-1}. The subsequent oxidation reaction to thiophene(O)(O) has an activation free energy of 39.7 kcal mol^{-1}.

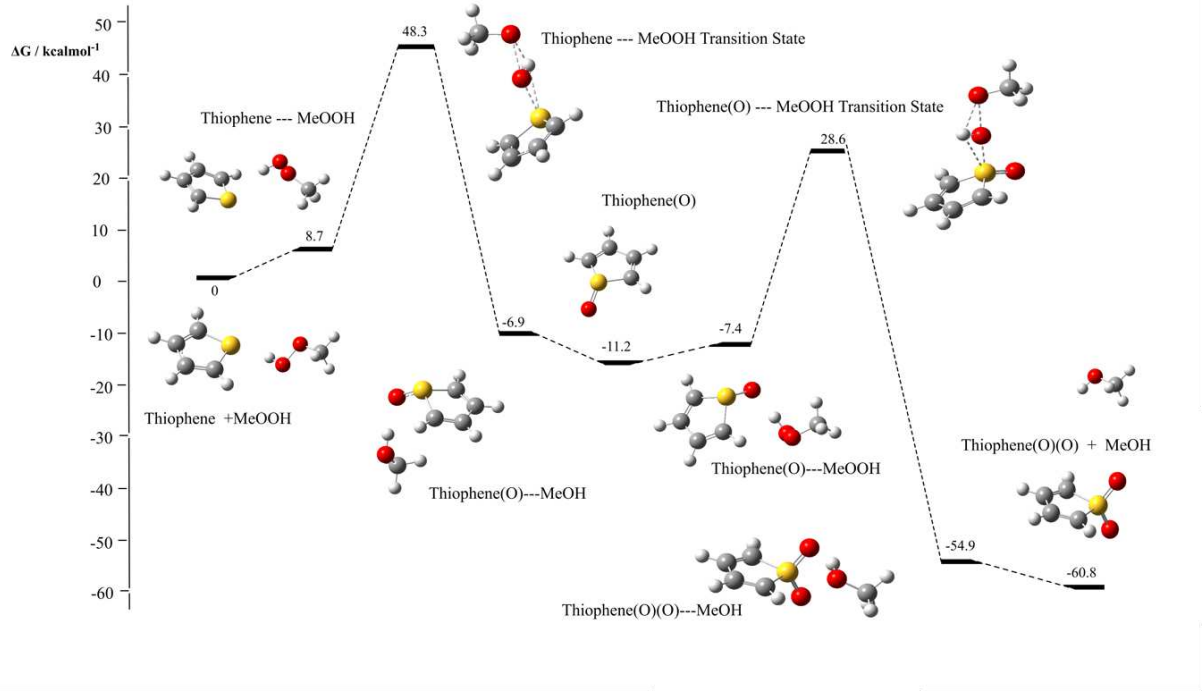

Figure 9: Gibbs free energy profile for the reaction of thiophene and MeOOH.

As can be seen in **Figures 10** and **11**, similar activation free energies were calculated for the reactions of both benzothiophene and dibenzothiophene with MeOOH. The calculated activation free energies for the first and second oxidation of benzothiophene are 44.8 and 40.3 kcal mol^{-1}. The first and second oxidation reactions of dibenzothiophenes have activation free energies of 43.2 and 40.7 kcal mol^{-1}.

The calculated activation free energies for the first reaction between hydroperoxides and each of thiophene, benzothiophene and dibenzothiophene are higher than those calculated for hexylsulfide. This is attributed to the loss in aromaticity during the oxidation.[55]

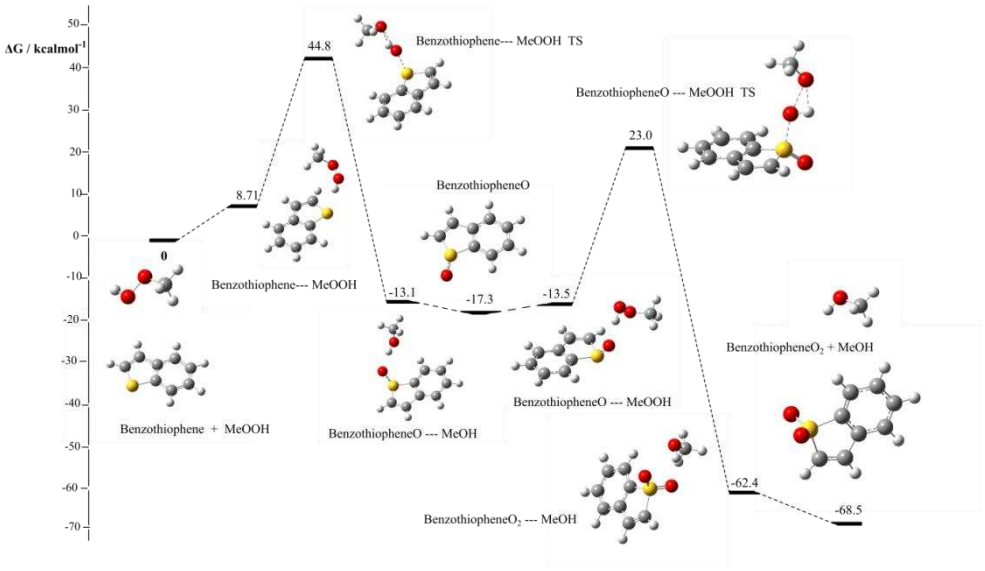

Figure 10: Gibbs free energy profile for the reaction of benzothiophene and MeOOH.

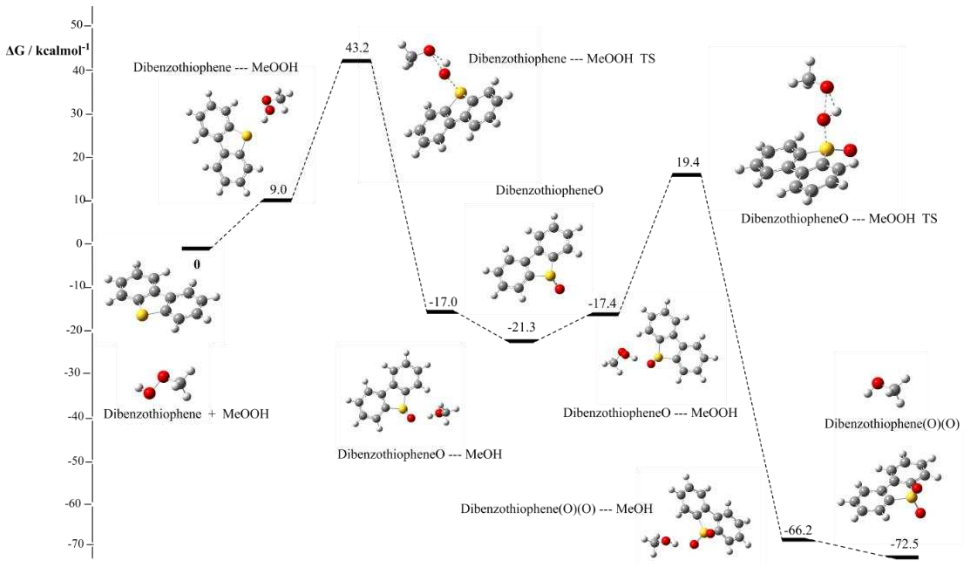

Figure 11: Gibbs free energy profile for the reaction of dibenzothiophene and MeOOH.

3.4 Reactions of disulfides

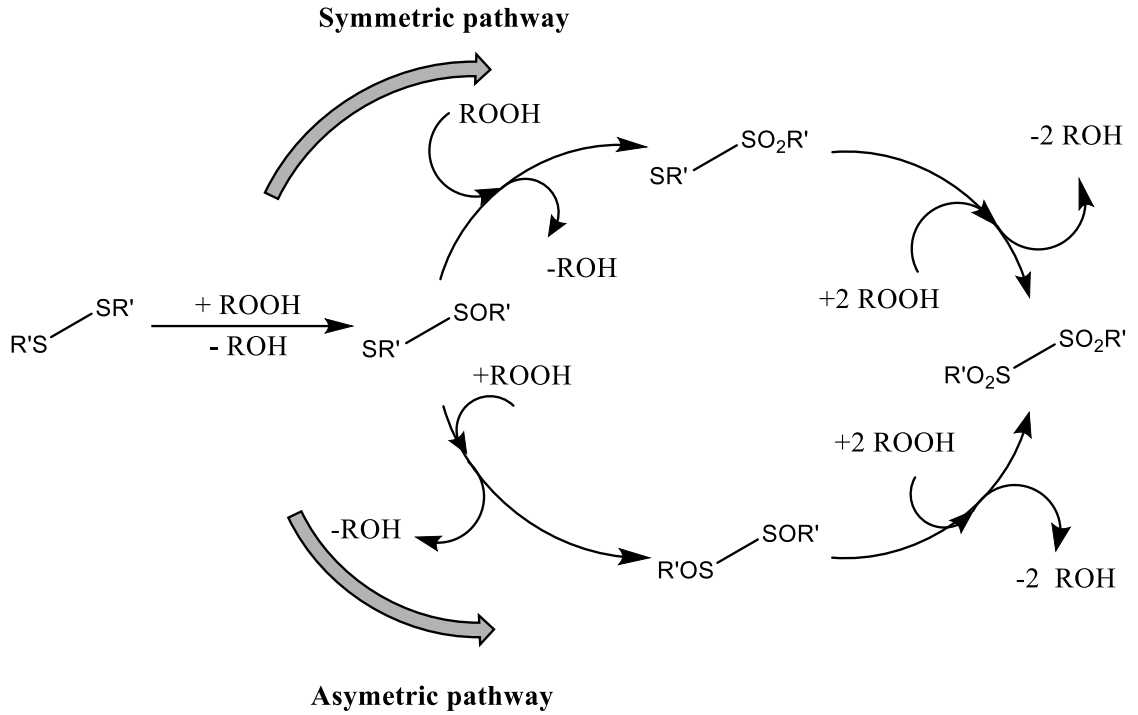

Scheme 2: Two potential mechanistic pathways leading to formation of RSO_2SO_2R.

Disulfides, with the general formula RSSR can potentially undergo as many as four oxidations with hydroperoxides. After the first oxidation, the second can occur at either the non-oxidized or oxidized sulfur atom as summarized in **Scheme 2**, leading to a second oxidation species that is either symmetric or asymmetric. However further oxidations will lead to the same end product.

The free energy profile for the reaction of dimethyldisulfide and MeOOH up to and including the second oxidation *via* the two different routes is shown in **Figure 12.** The initial oxidation has an activation energy of 38.5 kcal mol^{-1}, which is comparable to the activation free energy calculated for RSH oxidation in **Figure 8**. The activation free energies for the 2nd oxidation are 39.3 and 39.5 kcal mol^{-1} for symmetric and asymmetric oxidation respectively. This

indicates that there is almost no kinetic preference as to which sulfur atom will be oxidized after the initial oxidation

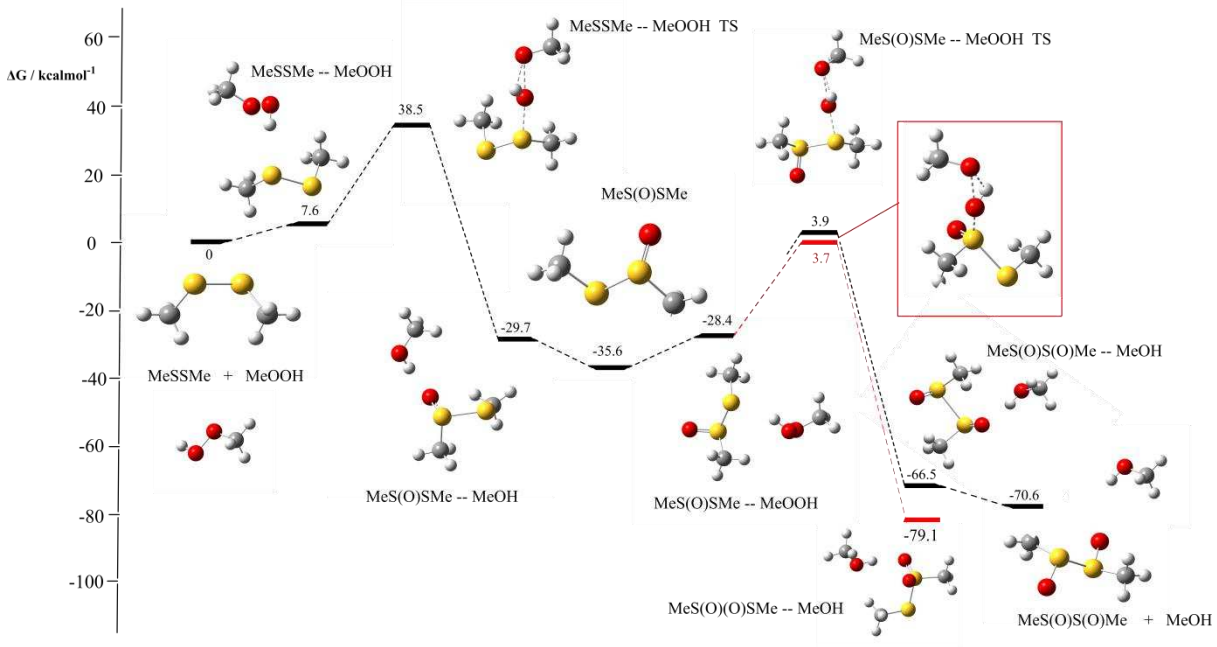

Figure 13: Gibbs free energy profile for the reaction of MeSSMe and MeOOH up to and including the second oxidation.

Corresponding activation free energies for the reaction of CHP and MeSSMe are 38.2 kcal mol^{-1} and 39.2 kcal mol^{-1} for the conversion of MeSSMe to MeS(O)SMe and MeS(O)SMe to MeS(O)S(O)Me respectively.

Oxidation is not the only reaction that disulfides can undergo. In particular, disulfides contain a diheteroatomic bond in much the same way as hydroperoxides and could potentially undergo a fission reaction to form two thiyl radical species which are known to be very reactive. Breaking of the disulfide bond will be easier if there is a significant weakening of the bond during the autoxidation process, as indicated by a lengthening of the S-S bond and consequentially change in the bond enthalpy.

The calculated bond enthalpies and corresponding S-S bond lengths for all of the potential species along the reaction coordinate are given in **Table 4.** The calculated S-S bond enthalpies for RSSR are 54 and 53 kcal mol^{-1} for R=Me and ^{n}Bu respectively. These values are comparable to literature values for disulfide bonds that are generally around 50-60 kcal mol^{-1}.[56] **Table 4** shows that the first and second oxidations appreciably weaken the disulfide bond. Therefore fission of the S-S bond under autoxidation conditions should be considered in more detail.

Table 4: S-S bond lengths and enthalpies for a series of disulfide species.

Disulfide species	**Bond enthalpy / kcal mol^{-1}**		**Bond Length / Å**	
	R = Me	R = ^{n}Bu	R = Me	R = ^{n}Bu
RSSR	54	53	2.068	2.092
RSOSR	32	32	2.167	2.235
RSOSOR	9	11	2.329	2.387
RSO_2SOR	18	18	2.310	2.389
RSO_2SO_2R	25	24	2.285	2.343

Our calculations show that the S-S bond significantly weakens upon successive oxidations. Even after a single oxidation, the activation free energy for the cleavage of the S-S bond becomes competitive with subsequent oxidations. Thus, the likely products from bond fission in these species are RSO● and RS●. Indeed, comparison with the activation free energy for RS(O)S(O)R formation, it is as likely to undergo bond fission than react with hydroperoxide. This is further substantiated by comparison of the frequency factors for both reactions (1.2E+22 for bond fission and 1.8E+06 for the oxidation reaction). Whilst RSO_2● can potentially form, the weakness of the S-S bond in RSOSOR makes this unlikely. We note that RSO● and RS● are relatable to the radical species formed during hydroperoxide fission, RO● and HO●, which are known to have critical roles in the autoxidation mechanism in fuels. Thus, it was

investigated whether any of the radicals that could potentially originate from disulfide fission could react with the bulk fuel in a similar way to peroxy radicals.

The free energy profile for the reaction of MeSO● and MeS● with bulk fuel is shown in **Figure 13.** For comparison, an equivalent profile was calculated for the reaction of MeO● and bulk fuel. In these reactions, hexane was used as a model for the hydrocarbons typically found in jet fuel to reduce the computational cost of the calculations. This approach can be justified as the reduction in chain length is not expected to have a significant effect on the reaction at the C2 carbon in the chain based upon previous studies.[53]

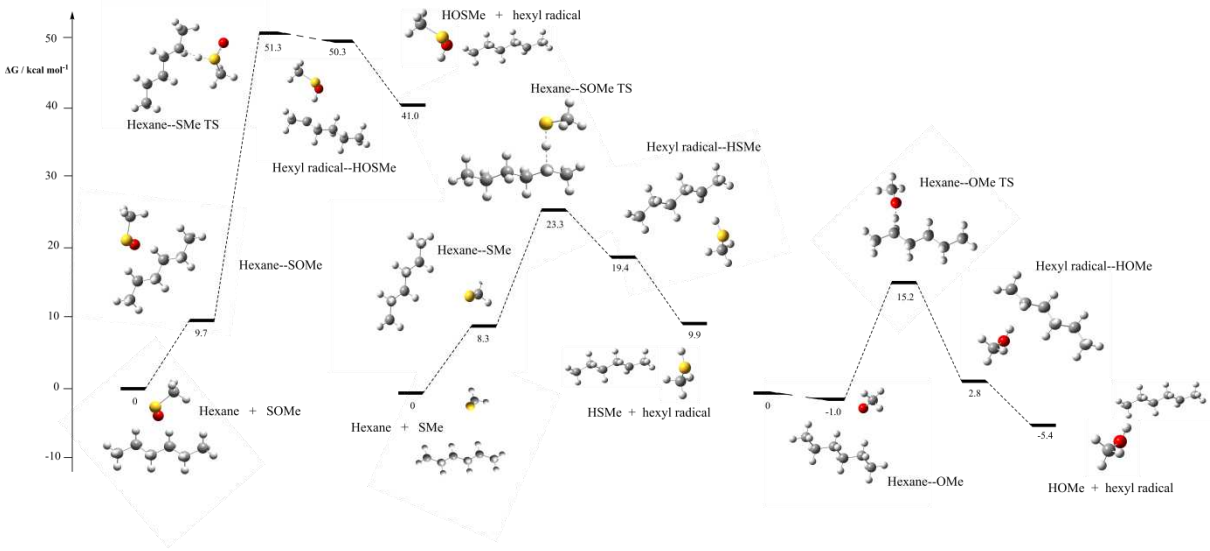

Figure 13: Gibbs free energy profile for the reaction of (left to right) MeS(O)●, MeS● and MeO● with hexane.

The activation free energies for the reaction of MeS●, MeS(O)● and MeO● with bulk fuel are calculated to be 51.3, 23.3 and 15.2 kcal mol^{-1}, respectively. Thus, the calculated activation free energy is appreciably larger for any of the sulfur species than for MeO●. Moreover, the reactions involving sulfur radicals are significantly endothermic. This indicates that the sulfur radical is better stabilized than a carbon radical.

In the above it was assumed that hydrogen abstraction happens through sulfur, i.e. that the radical character is localized there. However, a reaction could also happen through the oxygen atom. A comparison of the two energy profiles is shown in **Figure 14.**

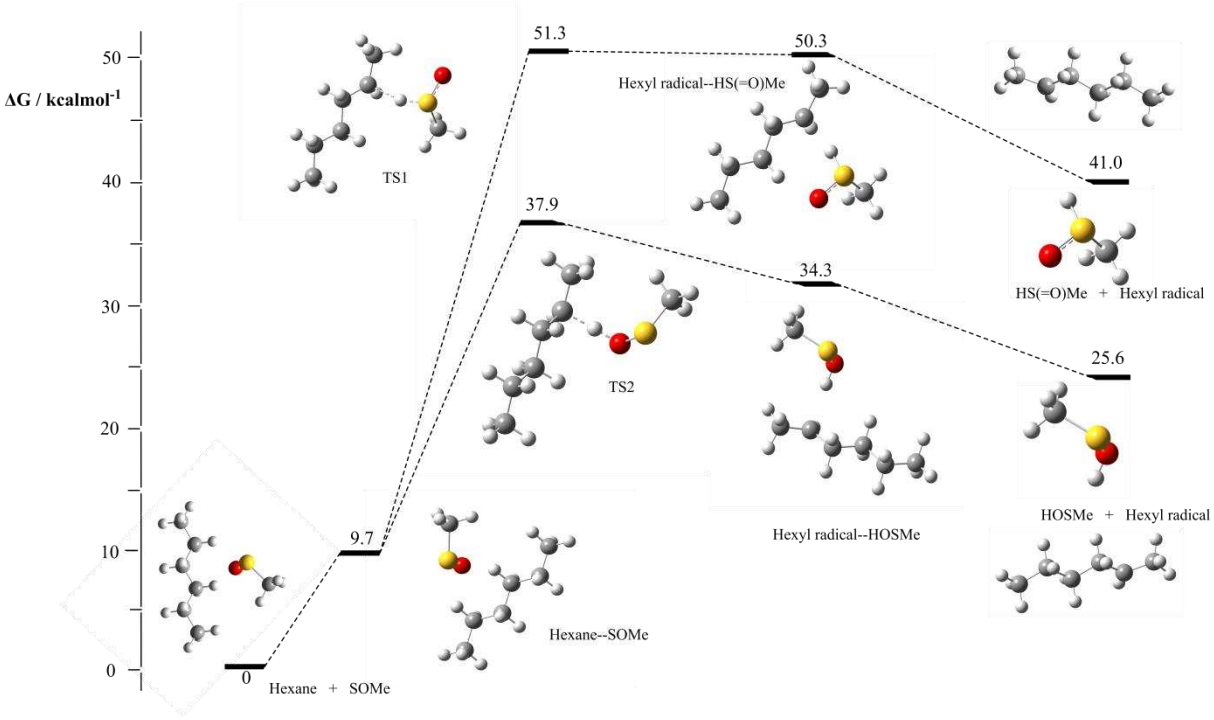

Figure 14: Gibbs free energy profile for the reaction of MeS(O)● and MeS●(O) with hexane.

As can be seen, abstraction by oxygen is preferred over sulfur (activation free energies 37.9 and 51.3 kcal mol^{-1}, respectively). However, even hydrogen abstraction by oxygen is still endothermic. Overall, the data in **Figures 13** and **14** suggest that any radical sulfur species formed from disulfide fission react less efficiently than radicals resulting from hydroperoxide fission.

Our final consideration was whether the thiyl radicals, MeS● and MeS(O)●, could potentially react with alcoholic species in the fuel. **Figure 15** shows the gibbs free energy profile for both reactions. The reaction of hexanol and MeS● has a low kinetic barrier and will be

surmountable given typical autoxidation conditions. In contrast, the reaction of hexanol and MeS(O)● has a significantly higher Gibbs free activation energy, which is likely to be prohibitive. In both cases, the reaction is endothermic, which suggests that the radical is better stabilized when localized on the sulfur of the respective thiyl radical than the oxygen on hexanol.

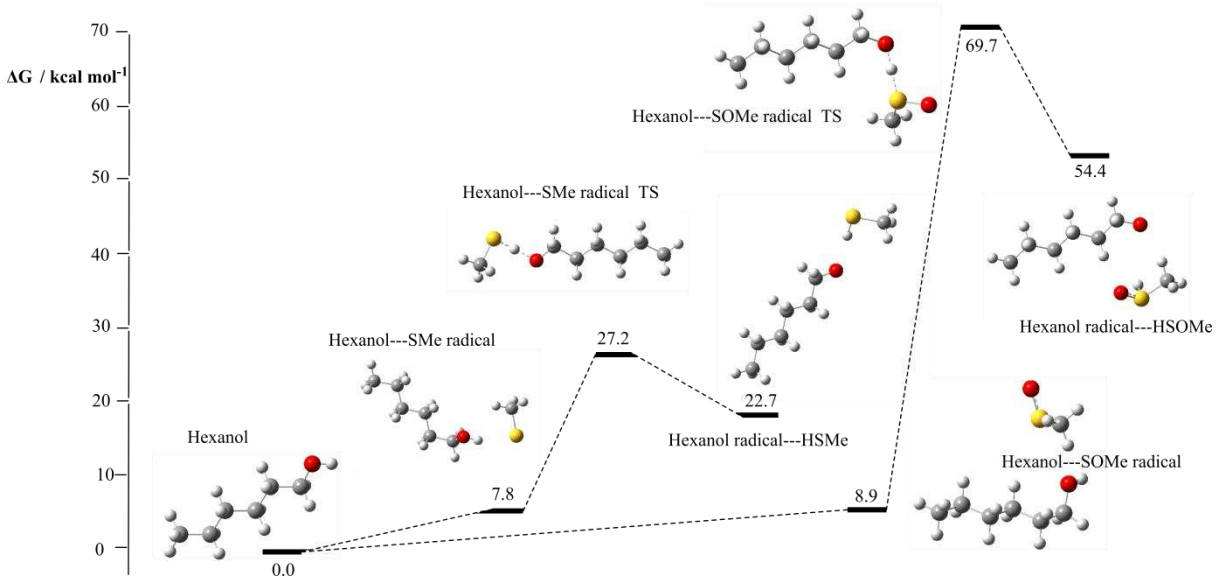

Figure 15: Gibbs free energy profile for the reaction of both MeS(O)● and MeS●(O) with hexanol.

3.5 Mechanistic implications

The work undertaken herein has provided greater insight into the elementary reactions involved in the oxidation of sulfur species. Oxidation of sulfur species can lead to the formation of alcohols, sulfones, sulfoxides and sulfonic acids. Moreover, cleavage of disulfides can form thiyl radicals.

The presence of various sulfur species in jet fuel has the potential to retard the rate of autoxidation by reacting with hydroperoxides. The larger data set, consisting of a range of sulfur species reacting with different hydroperoxides, provides a more robust framework for the improvement of current chemical kinetic models. As mentioned previously, these models are of great importance for predicting the rate of autoxidation in jet fuels. In the widely used Kuprowicz mechanism there is a single reaction where sulfur is involved, which does not differentiate between the different classes of sulfur species in the fuel (equation 1).[10] This work would allow for the expansion of this single reaction into a series of reactions that not only differentiate between the classes of sulfur compounds but also the specific individual reactions that each one might undergo.

To more accurately represent the reactions that potentially could occur, we would propose supplementing equation 1 in the current kinetic mechanism with the reactions outlined in **Table 5,** using the lumped data in **Table 6**. Reactions 1 to 4 describe the reactions of thiols and hydroperoxides. Reactions 5 and 6 describe the reactions of both thiophenes and sulfides with hydroperoxides. The reactions of disulfides and hydroperoxides are described by reactions 7-10.

462 **Table 5**: Proposed elementary steps to improve current chemical kinetic mechanisms

Elementary reaction step			Label
RSH + ROOH	⟶	RSHO + ROH	Reaction 1
RSHO + ROOH	⟶	RSOH + ROOH	Reaction 2
RSOH + ROOH	⟶	RSO_2H + ROH	Reaction 3
RSO_2H + ROOH	⟶	RSO3H + ROH	Reaction 4
RSR + ROOH	⟶	RSOR + ROH	Reaction 5
RSOR + ROOH	⟶	RSO_2R + ROH	Reaction 6
RSSR + ROOH	⟶	RSOSR + ROH	Reaction 7
RSOSR + ROOH	⟶	RSOSOR + ROH	Reaction 8
RSOSOR + ROOH	⟶	RSO_2SOR + ROH	Reaction 9
RSO_2SOR + ROOH	⟶	RSO_3SO_3R + ROH	Reaction 10

463

464 The reactions, lumped activation energies and Arrhenius data for the elementary reactions
465 investigated herein are summarized in **Table 6.** With appropriate validation against
466 experimental data and testing to deduce the importance of each individual reaction, it is hoped
467 that this data will lead to a more accurate chemical kinetic model for fuel autoxidation.

468

469 **Table 6.** Lumped data for proposed steps to improve current chemical kinetic mechanisms.

470 (COH = Cumene hydroxide)

Sulfur species (Hydroperoxide)	Elementary reaction step			E_a kcal mol^{-1}	*A* $mol^{-1}s^{-1}$	Source
	SH + R'OOH	⟶	$Products_{\cancel{SH}}$	18	3E+09	Ref 10
Thiols (MeOOH)	RSH + MeOOH	⟶	RSHO + MeOH	41.6	7.8E+05	This work
	RSHO + MeOOH	⟶	RSOH + MeOOH	19.2	4.0E+09	This work
	RSOH + MeOOH	⟶	RSO_2H + MeOH	31.0	5.1E+09	This work
	RSO_2H + MeOOH	⟶	RSO_3H + MeOH	38.9	1.9E+11	This work
Thiols (CHP)	RSH + CHP	⟶	RSHO + COH	40.9	2.9E+05	This work
	RSHO + CHP	⟶	RSOH + CHP	23.9	1.9E+07	This work
	RSOH + CHP	⟶	RSO_2H + COH	33.9	6.0E+08	This work
	RSO_2H + CHP	⟶	RSO_3H + COH	41.1	1.9E+09	This work
Thiols (^{t}BuOOH)	RSH + ^{t}BuOOH	⟶	RSHO + ^{t}BuOH	42.4	3.6E+05	This work
	RSHO + ^{t}BuOOH	⟶	RSOH + ^{t}BuOOH	20.2	3.5E+10	This work
	RSOH + ^{t}BuOOH	⟶	RSO_2H + ^{t}BuOH	33.7	2.9E+10	This work
	RSO_2H + ^{t}BuOOH	⟶	RSO_3H + ^{t}BuOH	42.3	3.0E+11	This work
Sulfides (MeOOH)	RSR + MeOOH	⟶	RSOR + MeOH	36.9	9.6E+06	This work
	RSOR + MeOOH	⟶	RSO_2R + MeOH	37.3	2.3E+09	This work
Sulfides	RSR + CHP	⟶	RSOR + COH	36.7	6.8E+05	This work

(CHP)	RSOR + CHP ⟶	RSO_2R + COH	37.4	E+08	This work
Sulfides	RSR + ^{t}BuOOH ⟶	RSOR + ^{t}BuOH	37.9	6.8E+05	This work
(^{t}BuOOH)	RSOR + ^{t}BuOOH ⟶	RSO_2R + ^{t}BuOH	39.6	2.2E+08	This work
Disulfides	RSSR + MeOOH ⟶	RSOSR + MeOH	39.9	6.5E+04	This work
(MeOOH)	RSOSR + MeOOH ⟶	RSOSOR + MeOH	39.3	1.3E+06	This work
	RSOSOR + MeOOH ⟶	RSO_2SOR + MeOH	34.3	2.0E+09	This work
	RSO_2SOR + MeOOH ⟶	RSO_3SO_3R + MeOH	38.3	1.1E+08	This work
Disulfides	RSSR + CHP ⟶	RSOSR + COH	41.9	1.3E+05	This work
(CHP)	RSOSR + CHP ⟶	RSOSOR + COH	41.6	3.8E+06	This work
	RSOSOR + CHP ⟶	RSO_2SOR + COH	36.6	8.0E+06	This work
	RSO_2SOR + CHP ⟶	RSO_3SO_3R + COH	38.9	1.4E+06	This work
Disulfides	RSSR + ^{t}BuOOH ⟶	RSOSR + ^{t}BuOH	39.8	5.8E+04	This work
(^{t}BuOOH)	RSOSR + ^{t}BuOOH ⟶	RSOSOR + ^{t}BuOH	40.6	5.4E+06	This work
	RSOSOR + ^{t}BuOOH ⟶	RSO_2SOR + ^{t}BuOH	35.2	8.5E+06	This work
	RSO_2SOR + ^{t}BuOOH ⟶	RSO_3SO_3R + ^{t}BuOH	38.9	2.2E+06	This work
Thiophenes and	RSR + MeOOH ⟶	RSOR + MeOH	45.4	8.3E+04	This work
Benzothiophenes	RSOR + MeOOH ⟶	RSO_2R + MeOH	40.8	4.6E+09	This work
(MeOOH)					
Thiophenes and	RSR + CHP ⟶	RSOR + COH	47.6	1.3E+04	This work
Benzothiophenes	RSOR + CHP ⟶	RSO_2R + COH	39.9	7.6E+08	This work
(CHP)					
Thiophenes and	RSR + ^{t}BuOOH ⟶	RSOR + ^{t}BuOH	46.3	1.2E+04	This work
Benzothiophenes	RSOR + ^{t}BuOOH ⟶	RSO_2R + ^{t}BuOH	41.6	4.3E+08	This work
(^{t}BuOOH)					

4 Conclusions

In this work, we have reported on the reactions of a series of sulfur compounds with model hydroperoxides for those found in jet fuel. Thiols can react with up to four equivalents of peroxides *via* a sulfenic acid to form sulfonic acids and alcohols. In contrast, sulfides can only react with two equivalents of peroxides and form sulfones as opposed to sulfonic acids.

The reaction of disulfide species with hydroperoxides generally have a higher activation energy compared to thiols and sulfides. These sulfur species can potentially react with multiple equivalents of peroxides to form sulfones. Each successive oxidation acts to weaken the sulfur-sulfur bond, which facilitates the homolytic fission reaction to form thiyl radicals. Our results indicate that these radicals do not favourably react with bulk fuel components

Once appropriately validated, current chemical kinetic models for the autoxidation of jet fuel will be improved with the inclusion of the more detailed individual reactions investigated here. This flexibility will also allow tailoring of the kinetic scheme to account for specific species of sulfur present in specific fuels.

Supporting Information

Cartesian coordinates for DFT-optimized structures. Raw GC data resulting from the speciation analysis. Collated thermochemical data for all species investigated.

Author information

Corresponding Author

Christopher Parks − Department of Mechanical Engineering, The University of Sheffield, Sheffield S3 7RD, U.K.; orcid.org/0000-0001-8016-474X; Email: c.m.parks@ sheffield.ac.uk

Authors

Anthony J. H. M. Meijer - Department of Chemistry, The University of Sheffield, Sheffield, S3 7HF.; orcid.org/ 0000-0003-4803-3488

Simon. Blakey - Department of Mechanical Engineering, The University of Birmingham, Birmingham B15 2TT, U.K.

Ehsan Alborzi − Department of Mechanical Engineering, The University of Sheffield, Sheffield S3 7RD, U.K.; orcid.org/ 0000-0002-2585-0824

Mohamed Pourkashanian − Department of Mechanical Engineering, The University of Sheffield, Sheffield S3 7RD, U.K.

Acknowledgments

The research presented in this paper has been performed in the framework of the JETSCREEN project (JETfuel SCREENING and optimization) and has received funding from the European Union Horizon 2020 Programme under grant agreement n◦ 723525. The authors declare no competing financial interest.

References

1. Balster, L. M.; Zabarnick, S.; Striebich, R. C.; Shafer, L. M.; West, Z. J., Analysis of Polar Species in Jet Fuel and Determination of Their Role in Autoxidative Deposit Formation. *Energy & Fuels* **2006,** *20*, 2564−2571.

2. Taylor, W. F., Deposit Formation from Deoxygenated Hydrocarbons. II. Effect of Trace Sulfur Compounds. *Product R&D* **1976,** *15* (1), 64-68.

3. Zabarnick, S.; Mick, M. S., Inhibition of Jet Fuel Oxidation by Addition of Hydroperoxide-Decomposing Species. *Ind. Eng. Chem. Res.* **1999,** *38*, 3557−3563.

4. Ervin, J. S.; Williams, T. F., Dissolved Oxygen Concentration and Jet Fuel Deposition. *Ind. Eng. Chem. Res.* **1996,** *35*, 899−904.

5. Grinstead, B.; Zabarnick, S., Studies of Jet Fuel Thermal Stability, Oxidation, and Additives Using an Isothermal Oxidation Apparatus Equipped with an Oxygen Sensor. *Energy & Fuels* **1999,** *13*, 756−760.

6. Jones, E. G.; Balster, L. M., Impact of Additives on the Autoxidation of a Thermally Stable Aviation Fuel. *Energy & Fuels* **1997,** *11*, 610-614.

7. Striebich, R. C.; Contreras, J.; Balster, L. M.; West, Z.; Shafer, L. M.; Zabarnick, S., Identification of Polar Species in Aviation Fuels using Multidimensional Gas Chromatography-Time of Flight Mass Spectrometry. . *Energy & Fuels* **2009,** *23*, 5474−5482.
8. Taylor, W. F.; Frankenfeld, J. W., Deposit Formation from Deoxygenated Hydrocarbons. 3. Effects of Trace Nitrogen and Oxygen Compounds. *Ind. Eng. Chem. Prod. Res. Dev.* **1978,** *17*, 86−90.
9. Zabarnick, S.; West, Z. J.; Shafer, L. M.; Mueller, S. S.; Striebich, R. C.; Wrzesinski, P. J., Studies of the Role of Heteroatomic Species in Jet Fuel Thermal Stability: Model Fuel Mixtures and Real Fuels. *Energy & Fuels* **2019,** *33* (9), 8557-8565.
10. Kuprowicz, N. J.; Zabarnick, S.; West, Z. J.; Ervin, J. S., Use of Measured Species Class Concentrations with Chemical Kinetic Modeling for the Prediction of Autoxidation and Deposition of Jet Fuels. *Energy & Fuels* **2007,** *21* (2), 530-544.
11. Pickard, J. M.; Jones, E. G., Catalysis of Jet-A Fuel Autoxidation by Fe2O3. *Energy & Fuels* **1997,** *11*, 1232−1236.
12. West, Z. J.; Zabarnick, S.; Striebich, R. C., Determination of Hydroperoxides in Jet Fuel via Reaction with Triphenylphosphine. *Industrial & Engineering Chemistry Research* **2005,** *44* (10), 3377-3383.
13. Zabarnick, S., Chemical kinetic modeling of jet fuel autoxidation and antioxidant chemistry. *Industrial & Engineering Chemistry Research* **1993,** *32* (6), 1012-1017.
14. Aksoy, P.; Gül, Ö.; Cetiner, R.; Fonseca, D. A.; Sobkowiak, M.; Falcone-Miller, S.; Miller, B. G.; Beaver, B., Insight into the Mechanisms of Middle Distillate Fuel Oxidative Degradation. Part 2: On the Relationship between Jet Fuel Thermal Oxidative Deposit, Soluble Macromolecular Oxidatively Reactive Species, and Smoke Point. *Energy & Fuels* **2009,** *23* (4), 2047-2051.
15. Ben Amara, A.; Kaoubi, S.; Starck, L., Toward an optimal formulation of alternative jet fuels: Enhanced oxidation and thermal stability by the addition of cyclic molecules. *Fuel* **2016,** *173*, 98-105.
16. Chatelain, K.; Nicolle, A.; Ben Amara, A.; Catoire, L.; Starck, L., Wide Range Experimental and Kinetic Modeling Study of Chain Length Impact on n-Alkanes Autoxidation. *Energy & Fuels* **2016,** *30* (2), 1294-1303.
17. Galano, A.; Alvarez-Idaboy, J. R., Kinetics of radical-molecule reactions in aqueous solution: A benchmark study of the performance of density functional methods. *Journal of Computational Chemistry* **2014,** *35* (28), 2019-2026.
18. Gül, Ö.; Cetiner, R.; Griffith, J. M.; Wang, B.; Sobkowiak, M.; Fonseca, D. A.; Aksoy, P.; Miller, B. G.; Beaver, B., Insight into the Mechanisms of Middle Distillate Fuel Oxidative Degradation. Part 3: Hydrocarbon Stabilizers to Improve Jet Fuel Thermal Oxidative Stability. *Energy & Fuels* **2009,** *23* (4), 2052-2055.

19. Jalan, A.; Alecu, I. M.; Meana-Pañeda, R.; Aguilera-Iparraguirre, J.; Yang, K. R.; Merchant, S. S.; Truhlar, D. G.; Green, W. H., New Pathways for Formation of Acids and Carbonyl Products in Low-Temperature Oxidation: The Korcek Decomposition of γ-Ketohydroperoxides. *Journal of the American Chemical Society* **2013,** *135* (30), 11100-11114.

20. Mangiatordi, G. F.; Brémond, E.; Adamo, C., DFT and Proton Transfer Reactions: A Benchmark Study on Structure and Kinetics. *Journal of Chemical Theory and Computation* **2012,** *8* (9), 3082-3088.

21. Park, S. H.; Kwon, C. H.; Kim, J.; Han, J. S.; Jeong, B. H.; Han, H.; Kim, S. H., Mechanistic Insights into Oxidative Decomposition of exo-Tetrahydrodicyclopentadiene. *The Journal of Physical Chemistry C* **2013,** *117* (31), 15933-15939.

22. Lobodin, V. V.; Robbins, W. K.; Lu, J.; Rodgers, R. P., Separation and Characterization of Reactive and Non-Reactive Sulfur in Petroleum and Its Fractions. *Energy & Fuels* **2015,** *29* (10), 6177-6186.

23. Link, D. D.; Baltrus, J. P.; Rothenberger, K. S.; Zandhuis, P.; Minus, D. K.; Striebich, R. C., Class- and Structure-Specific Separation, Analysis, and Identification Techniques for the Characterization of the Sulfur Components of JP-8 Aviation Fuel. *Energy & Fuels* **2003,** *17* (5), 1292-1302.

24. Stumpf, Á.; Tolvaj, K.; Juhász, M., Detailed analysis of sulfur compounds in gasoline range petroleum products with high-resolution gas chromatography–atomic emission detection using group-selective chemical treatment. *Journal of Chromatography A* **1998,** *819* (1), 67-74.

25. Batts, B. D.; Fathoni, A. Z., A literature review on fuel stability studies with particular emphasis on diesel oil. *Energy & Fuels* **1991,** *5* (1), 2-21.

26. de Souza, W. F.; Guimarães, I. R.; Guerreiro, M. C.; Oliveira, L. C. A., Catalytic oxidation of sulfur and nitrogen compounds from diesel fuel. *Applied Catalysis A: General* **2009,** *360* (2), 205-209.

27. Fathoni, A. Z.; Batts, B. D., A literature review of fuel stability studies with a particular emphasis on shale oil. *Energy & Fuels* **1992,** *6* (6), 681-693.

28. Kendall, D. R.; Clark, R. H.; Wolveridge, P. E., Fuels for Jet Engines: The Importance of Thermal Stability. *Aircraft Engineering and Aerospace Technology* **1987,** *59* (12), 2-7.

29. Mushrush, G. W.; Hazlett, R. N.; Pellenbarg, R. E.; Hardy, D. R., Role of sulfur compounds in fuel instability: a model study of the formation of sulfonic acids from hexyl sulfide and hexyl disulfide. *Energy & Fuels* **1991,** *5* (2), 258-262.

30. Zabarnick, S.; Phelps, D. K., Density Functional Theory Calculations of the Energetics and Kinetics of Jet Fuel Autoxidation Reactions. *Energy & Fuels* **2006,** *20* (2), 488-497.

602 31. Hiley, R. W.; Pedley, J. F., Storage stability of petroleum-derived diesel fuel: 2. The effect of
603 sulphonic acids on the stability of diesel fuels and a diesel fuel extract. *Fuel* **1988,** *67* (4), 469-473.
604 32. Offenhauer, R. D.; Brennan, J. A.; Miller, R. C., Sediment Formation in Catalytically Cracked
605 Distillate Fuel Oils. *Industrial & Engineering Chemistry* **1957,** *49* (8), 1265-1266.
606 33. Denison, G. H., Oxidation of Lubricating Oils. *Industrial & Engineering Chemistry* **1944,** *36* (5),
607 477-482.
608 34. Thompson, R. B.; Druge, L. W.; Chenicek, J. A., Stability of Fuel Oils in Storage: Effect of
609 Sulfur Compounds. *Industrial & Engineering Chemistry* **1949,** *41* (12), 2715-2721.
610 35. Daniel, S. R.; Heneman, F. C., Deposit formation in liquid fuels: 4. Effect of selected organo-
611 sulphur compounds on the stability of Jet A fuel. *Fuel* **1983,** *62* (11), 1265-1268.
612 36. Rawson, P. M.; Webster, R. L.; Evans, D.; Abanteriba, S., Contribution of sulfur compounds
613 to deposit formation in jet fuels at 140 °C using a quartz crystal microbalance technique. *Fuel* **2018,**
614 *231*, 1-7.
615 37. Bach, R. D.; Dmitrenko, O., Electronic Requirements for Oxygen Atom Transfer from Alkyl
616 Hydroperoxides. Model Studies on Multisubstrate Flavin-Containing Monooxygenases. *The Journal*
617 *of Physical Chemistry B* **2003,** *107* (46), 12851-12861.
618 38. Beens, J.; Tijssen, R., The characterization and quantitation of sulfur-containing compounds
619 in (heavy) middle distillates by LC-GC-FID-SCD. *Journal of High Resolution Chromatography* **1997,** *20*
620 (3), 131-137.
621 39. Ruiz-Guerrero, R.; Vendeuvre, C.; Thiébaut, D.; Bertoncini, F.; Espinat, D., Comparison of
622 Comprehensive Two-Dimensional Gas Chromatography Coupled with Sulfur-Chemiluminescence
623 Detector to Standard Methods for Speciation of Sulfur-Containing Compounds in Middle Distillates.
624 *Journal of Chromatographic Science* **2006,** *44* (9), 566-573.
625 40. Wang, F. C.-Y.; Robbins, W. K.; Di Sanzo, F. P.; McElroy, F. C., Speciation of Sulfur-Containing
626 Compounds in Diesel by Comprehensive Two-Dimensional Gas Chromatography. *Journal of*
627 *Chromatographic Science* **2003,** *41* (10), 519-523.
628 41. M. J. Frisch; G. W. Trucks; H. B. Schlegel; G. E. Scuseria; M. A. Robb; J. R. Cheeseman; G.
629 Scalmani; V. Barone; B. Mennucci; G. A. Petersson; H. Nakatsuji; M. Caricato; X. Li; H. P.
630 Hratchian; A. F. Izmaylov; J. Bloino; G. Zheng; J. L. Sonnenberg; M. Hada; M. Ehara; K. Toyota; R.
631 Fukuda; J. Hasegawa; M. Ishida; T. Nakajima; Y. Honda; O. Kitao; H. Nakai; T. Vreven; J. A.
632 Montgomery, J.; J. E. Peralta; F. Ogliaro; M. Bearpark; J. J. Heyd; E. Brothers; K. N. Kudin; V. N.
633 Staroverov; T. Keith; R. Kobayashi; J. Normand; K. Raghavachari; A. Rendell; J. C. Burant; S. S.
634 Iyengar; J. Tomasi; M. Cossi; N. Rega; J. M. Millam; M. Klene; J. E. Knox; J. B. Cross; V. Bakken; C.
635 Adamo; J. Jaramillo; R. Gomperts; R. E. Stratmann; O. Yazyev; A. J. Austin; R. Cammi; C. Pomelli, J.

636 W. O.; R. L. Martin; K. Morokuma; V. G. Zakrzewski; G. A. Voth; P. Salvador; J. J. Dannenberg; S.
637 Dapprich; A. D. Daniels; O. Farkas; J. B. Foresman; J. V. Ortiz; J. Cioslowski; Fox, D. J. *Gaussian 09*,
638 2016.
639 42. Clint Whaley, R.; Petitet, A.; Dongarra, J. J., Automated empirical optimizations of software
640 and the ATLAS project. *Parallel Computing* **2001,** *27* (1), 3-35.
641 43. Whaley, R. C.; Petitet, A., Minimizing development and maintenance costs in supporting
642 persistently optimized BLAS. *Software: Practice and Experience* **2005,** *35* (2), 101-121.
643 44. Becke, A. D., Density-functional exchange-energy approximation with correct asymptotic
644 behavior. *Physical Review A* **1988,** *38* (6), 3098-3100.
645 45. Lee, C.; Yang, W.; Parr, R. G., Development of the Colle-Salvetti correlation-energy formula
646 into a functional of the electron density. *Physical Review B* **1988,** *37* (2), 785-789.
647 46. Perdew, J. P.; Chevary, J. A.; Vosko, S. H.; Jackson, K. A.; Pederson, M. R.; Singh, D. J.;
648 Fiolhais, C., Atoms, molecules, solids, and surfaces: Applications of the generalized gradient
649 approximation for exchange and correlation. *Physical Review B* **1992,** *46* (11), 6671-6687.
650 47. Dunning Jr., T. H., Gaussian basis sets for use in correlated molecular calculations. I. The
651 atoms boron through neon and hydrogen. *The Journal of Chemical Physics* **1989,** *90* (2), 1007-1023.
652 48. Cossi, M.; Barone, V., Analytical second derivatives of the free energy in solution by
653 polarizable continuum models. *The Journal of Chemical Physics* **1998,** *109* (15), 6246-6254.
654 49. Scalmani, G.; Frisch, M. J., Continuous surface charge polarizable continuum models of
655 solvation. I. General formalism. *The Journal of Chemical Physics* **2010,** *132* (11), 114110.
656 50. Cancès, E.; Mennucci, B.; Tomasi, J., A new integral equation formalism for the polarizable
657 continuum model: Theoretical background and applications to isotropic and anisotropic dielectrics.
658 *The Journal of Chemical Physics* **1997,** *107* (8), 3032-3041.
659 51. Funes-Ardoiz;, I.; Paton, R. S. GoodVibes: Version 2.0.3. Zenodo 2018.
660 52. Werner, H.-J.; Knowles, P. J.; Knizia, G.; Manby, F. R.; Schütz, M., Molpro: a general-
661 purpose quantum chemistry program package. *WIREs Computational Molecular Science* **2012,** *2* (2),
662 242-253.
663 53. Parks, C. M.; Alborzi, E.; Blakey, S. G.; Meijer, A. J. H. M.; Pourkashanian, M., Density
664 Functional Theory Calculations on Copper-Mediated Peroxide Decomposition Reactions: Implications
665 for Jet Fuel Autoxidation. *Energy & Fuels* **2020,** *34* (6), 7439-7447.
666 54. Alborzi, E.; Parks, C. M.; Gadsby, P.; Sheikhansari, A.; Blakey, S. G.; Pourkashanian, M.,
667 Effect of Reactive Sulfur Removal by Activated Carbon on Aviation Fuel Thermal Stability. *Energy &*
668 *Fuels* **2020,** *34* (6), 6780-6790.

669 55. Lu, Y.; Dong, Z.; Wang, P.; Zhou, H.-B., Thiophene Oxidation and Reduction Chemistry. In
670 *Thiophenes*, Joule, J. A., Ed. Springer International Publishing: Cham, 2015; pp 227-293.
671 56. Denk, M. K., The Variable Strength of the Sulfur–Sulfur Bond: 78 to 41 kcal – G3, CBS-Q, and
672 DFT Bond Energies of Sulfur (S8) and Disulfanes XSSX (X = H, F, Cl, CH3, CN, NH2, OH, SH). *European*
673 *Journal of Inorganic Chemistry* **2009,** *2009* (10), 1358-1368.

674